



Study on the effect of pressure and cooling rate on the solidification Characteristics and mechanical properties of Al-11%Si cast alloy

H. Barhoumi^{1,2*}, S. Souissi¹, M. Ben Amar¹, F. Elhalouani¹

¹ Laboratory LASEM, National Engineering School of Sfax, National Engineering School of Sfax (ENIS), University of Sfax, B.P 599-3038, Tunisia.

² Faculty of Sciences of Sfax (FSS), University of Sfax, B.P 802-3038, Tunisia

Received 14 March 2019,
Revised 15 Aug 2019,
Accepted 16 Aug 2019

Keywords

- ✓ Al-11%Si alloy,,
- ✓ Differential Thermal Analysis (DTA),
- ✓ pressure,
- ✓ cooling rate,
- ✓ microstructure,
- ✓ mechanical properties.

hendabarhoumi@yahoo.fr;
Phone: +216 411609264

Abstract

The effect of various cooling rates which was achieved by means of squeeze casting samples on microstructure and solidification of Al-11%Si cast alloy has been investigated. Investigations have been made by Differential Thermal Analysis (DTA) and metallographic Analysis. For this purpose, the solidification process was studied using the cooling curve and crystallization curve at solidification rate ranging from 5 k/min up to 99 k/min. The results show that, during the solidification at different cooling rates, the undercooling and recalescence of primary and eutectic crystallization have been detected and related with largeness of primary crystals of α (Al) and eutectic phase β (Si) from eutectic (α Al + β Si). Increasing the cooling rate increases significantly the liquidus temperature, nucleation undercooling temperature, solidification range and decreases the undercooling temperature. Therefore, increasing cooling rate refines all microstructural features including secondary dendrite arm spacing (SDAS) intermetallic compounds thus improves mechanical properties.

1. Introduction

Due to different excellent advantages such as high fluidity, wettability, formability, high specific strength, shrinkage reduction, excellent corrosion resistance, low thermal expansion co-efficient, wear resistance, good mechanical properties and castability, the aluminum silicon alloys is widely used as casting material in the foundry [1-3]. Among these alloys, eutectic and hypereutectic alloys are really attractive for their wear resistance properties, low density, abrasion resistance and low cost. They also improve fluidity, reduce melting temperature and are easily available. They are converted to ideal alloys to manufacture the automobile parts [4, 5]. Thus, these alloys have become increasingly important in recent years thanks to their different advantages.

In recent years, a new forming technology for improved alloy properties: squeeze casting, has been developed. The research focused on use of advanced squeeze casting processes which combine the features of both casting and forging processes. This process consists of solidifying the alloy under a certain applied pressure that is maintained until the end of solidification. Consequently, casting soundness and mechanical properties are improved.

It is well known that squeeze pressure decreased the percentage of porosity and increased density as well as grain size. It is often observed that grain size depends on solidification rate during casting. In fact the combination of high pressures and metal molds leads to high heat transfer coefficients which in turn lead to a refinement of microstructure [6–8]. Skolianos et al. reported the effect of squeeze pressure on mechanical and microstructure properties of squeeze cast AA6061aluminium alloy [9]. Fan et al. have investigated the effects of casting temperatures on ultimate tensile strengths and micro-structure properties such as grain size and secondary

dendrite arm spacing (SDAS) of squeeze cast Al-Zn-Mg-Cu alloy [10]. Similarly, El-khair found that squeeze pressures decrease the percentage of porosity and the grain size of α -Al and modify the Si eutectic [11]. 2024 Al alloy is studied by Hajjari and Divandari [12] and was reported to have brought about a higher cooling rate and lower secondary dendrite arm spacing (SDAS). Also in alloying elements [13] and heat treatment [14], higher cooling rates have strongly affected the mechanical properties and microstructure of near eutectic Al-Si alloys [6, 15].

The cooling rate is one of the most important variables which affect the structure of as-cast alloy. More than 300 series alloys have been investigated by many authors [16-19]. According to their research, high cooling rate decreases grain size, the dendrite arm spacing (DAS), intermetallic phases and shrinkage porosity [2]. It also causes more uniform distribution of porosity. Also, it modifies the size of constituents' structure (primary and eutectic silicon); it decreases the size of them. Easton and StJohn [20] analyzed the influence of cooling rate on the grain size of Al alloys and correlate their observations with the increasing number of nuclei and restriction factor. They found that the cooling rates have an impact on the grain refinement. However, changes in phase nucleation temperatures, nucleation, undercooling and solidification ranges with increasing cooling rates have not been extensively investigated in the literature.

Various researchers have focused on the effect of the cooling rate on microstructural features and mechanical properties. Radha krishna et al [17-21] explored that DAS for different alloys is linearly related to solidification time, temperature gradient, freezing index and non-linearly to the ultimate tensile strength (UTS), yield strength (YS) and ductility. Different levels of silicon content also have an effect on the effectiveness of grain refiner. Lee et al. [22] discovered that the effectiveness of grain refiner is better before the transition point (about 3% silicon content in unrefined alloy) and the grain size remain the same regardless the amount of refiner added to the alloy.

The Thermal analysis (TA) is based on the fact that the thermal events on a heating or cooling curve are directly related to the transformation's phase occurring in a sample. The temperature changes in the material are recorded as a function of the heating or cooling time in such a manner that allows are detected in the transformations' phase. The cooling curves of the thermal analysis can accurately determine the characteristics solidification temperatures and microstructure [23, 24].

Many measurement techniques are available to investigate the solidification of metals and alloys. Such as Differential Thermal Analysis (DTA), Differential Scanning Calorimetry (DSC) and computer aided cooling curve analysis (CA-CCTA). These are all very accurate and well documented; they are inadequate for industries to investigate solidification of metals and alloys [23]. In this research, the DTA technique was used.

The DTA has more sensitivity and reliability compared to conventional thermal analysis because it employs a reference sample that does not undergo any phase change in the investigated temperature range. The temperature differences between the test sample and reference sample are accurately measured during controlled cooling or heating cycles. The resolution of DTA instruments is generally very high, which makes this instrument useful for many research applications [23].

The purpose of the present work is to investigate, the influence of pressure and cooling rates was carried out on cast aluminum alloy Al-11%Si. The solidification characteristics and precipitation behavior obtained under different squeeze pressures and cooling rates conditions by using DTA technique were also investigated to provide theoretical support for the evolution of strength. This is to find the relationship between the microstructure of alloy and the mechanical properties under the different conditions.

2. Material and Methods

2.1. Material

The experiments were carried out using an Al-11%Si aluminum die casting alloy. Due to different advantage the material is purchased commercially and widely used in mechanical applications. The chemical composition (mass fraction) is shown in Table 1.

2.2. Squeeze casting process

The material was melted in an electrical resistance furnace. The melt temperature was kept at 750°C for 60 minutes, in the cast mold preheated to 250 °C. The squeeze casting experiment was performed on a hydraulic

press consisting of steel mould, where the pressure on the molten metal was kept constant until the end of solidification. In gravity casting, the molten metal was poured directly into the mould without external pressure.

Table1: Average chemical composition (wt %) of investigated alloy, and cooling rate – CR and heating rate – HR

Si	Mg	Mn	Ni	Fe	Cu	Cr	Zn	Al	CR (K/min)	HT (K/min)
11.1	0.11	0.06	0.1	0.29	0.09	0.03	0.15	Rest.	5	2
									15	5
									99	15

The device is also equipped with a system which provides temperature regulation of the mould. The punch-and-die set were made of hot-die steel and the cast billets were cylindrical in shape of 23 mm in diameter and 120 mm in length. Three pressures were tested: 0, 40, 80 and 110 MPa. A delay time of 15 s between the melt injection and the squeeze beginning was kept. Pressure was applied for 30 s and the sample was extracted after its complete solidification.

2.3. Differential thermal analysis

Specimens were then machined into rods of approximately 3.9 mm in diameter and 6 mm in height, and then subjected to DTA using SETARAM –SETSYS apparatus. All experiments were carried out under a low argon flux. The DTA signals were recorded with scanning rates for heating of 2, 5 and 15 (K/min) and for cooling of 5, 15 and 99 (K/min). At the end of heating, the samples were held at upper temperature of 650 °C for 10 min. Each run was made twice for having samples for metallographic and for tomographic investigation. The DTA samples were prepared for metallographic observation was performed by the scanning electron microscope (SEM) LEO 435VP.

2.3. Secondary dendrite arm spacing measurement

SDAS measurement is of paramount importance in deciding the mechanical properties and is influenced by the major parameters namely liquid metal treatment, solidification time, temperature gradient between the metal-mould interfaces and alloy chemical composition. Linear intercept method was used for the measurement of SDAS via image analysis software. The quantification of SDAS is done by drawing the lines measuring the distance between the adjacent sides on the longitudinal part of a primary dendrite as a function of the distance from the dendrite tip [25].

3. Results and discussion

3.1. Effect of pressures on solidification behavior of Al-11%Si.

Figure 1 shows the microstructure of gravity die casting and squeeze casting of Al-11%Si alloy obtained from different pressure levels at 15 (K/min) cooling rate. It can be seen that the microstructure of the squeeze casting and the gravity casting was fully dendritic of α -Al. (light grey- Fig.1a), eutectic silicon phase (dark grey- Fig.1b), and different intermetallic phases. They can be identified by two important phases: Fe-rich phases (β -Al₃FeSi) and Cu-rich phases (θ -Al₂Cu). By applying pressure, the microstructure becomes finer, homogenous and smaller in size. This change results from greater cooling rates for the solidifying alloy can be realized due to reduction in the air gap between the melt and the die wall. Thus, increase of the solidification rate and decrease of dendrite arm spacing (DAS). The microstructure configurations for other cooling rates were similar. By melting and freezing an alloy and registering the temperature time curves, several characteristic behaviors can be determined [26].

During the solidification of Al-11%Si cast alloy, three different reactions occur successively at decreasing temperature. At first, the solidification commenced with precipitation of primary silicon phase at 570°C (refer to point 1 in figure 2). Then it progressed with formation of the (α (Al) + β (Si)) eutectic at 562°C (point 2). Finally,

at 542°C the solidification of β intermetallic phase was detected at the end of solidification process on the DTA cooling curves (point 3). Solidification was completed at 522°C [27-28].

The DTA curves of gravity casting and squeeze casting of as-cast Al-11%Si alloy samples under different pressures ranging from 40 to 110 MPa are shown in Figure 3. It can be seen that the melting curves at a heating rate of 2 K/min, 5 K/min and 15 K/min are not quite clear compared to those cooling rate of 5 K/min, 15 K/min and 99 K/min of all pressures particularly at the beginning of melting of the eutectic phase mixture.

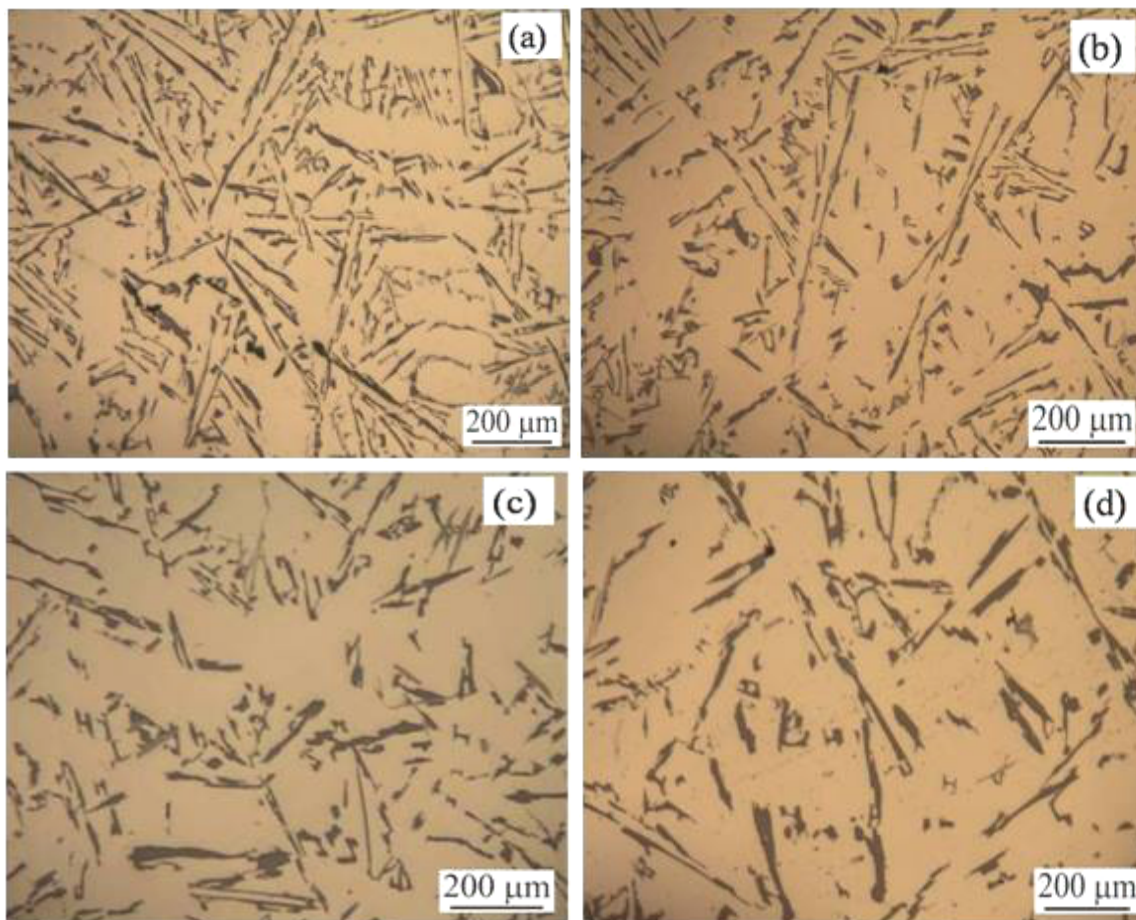


Fig.1: Micrographs of DTA samples solidified at the cooling rate 15 K/min of various pressures (a) 0 MPa, (b) 40 MPa, (c) 80 MPa (d) 110 MPa.

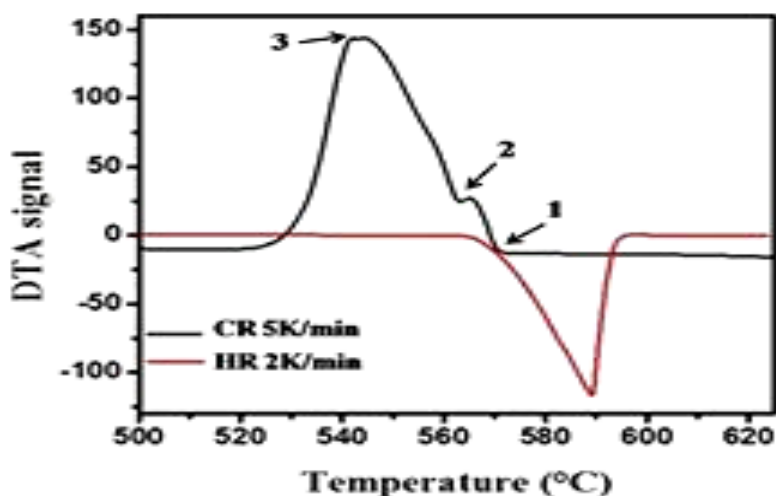


Fig.2: DTA analysis of heating and cooling rates at the speed of 2 and 5 K/min of gravity cast (P=0 MPa).

Also, on the DTA curves of gravity castings there are two exothermic peaks. With increasing pressure, the same peak becomes smaller. Firstly, peak 1 corresponding to eutectic reaction became smaller with the increase of pressure, and eventually disappeared when the increase of pressure 110MPa and cooling rate at 99 K/min. Secondly, with the increase of specific pressure and cooling rate the exothermic peak 2 appeared clearly (see Figs.2 and 3). The temperatures of exothermic peaks on DTA curves are listed in Table 2.

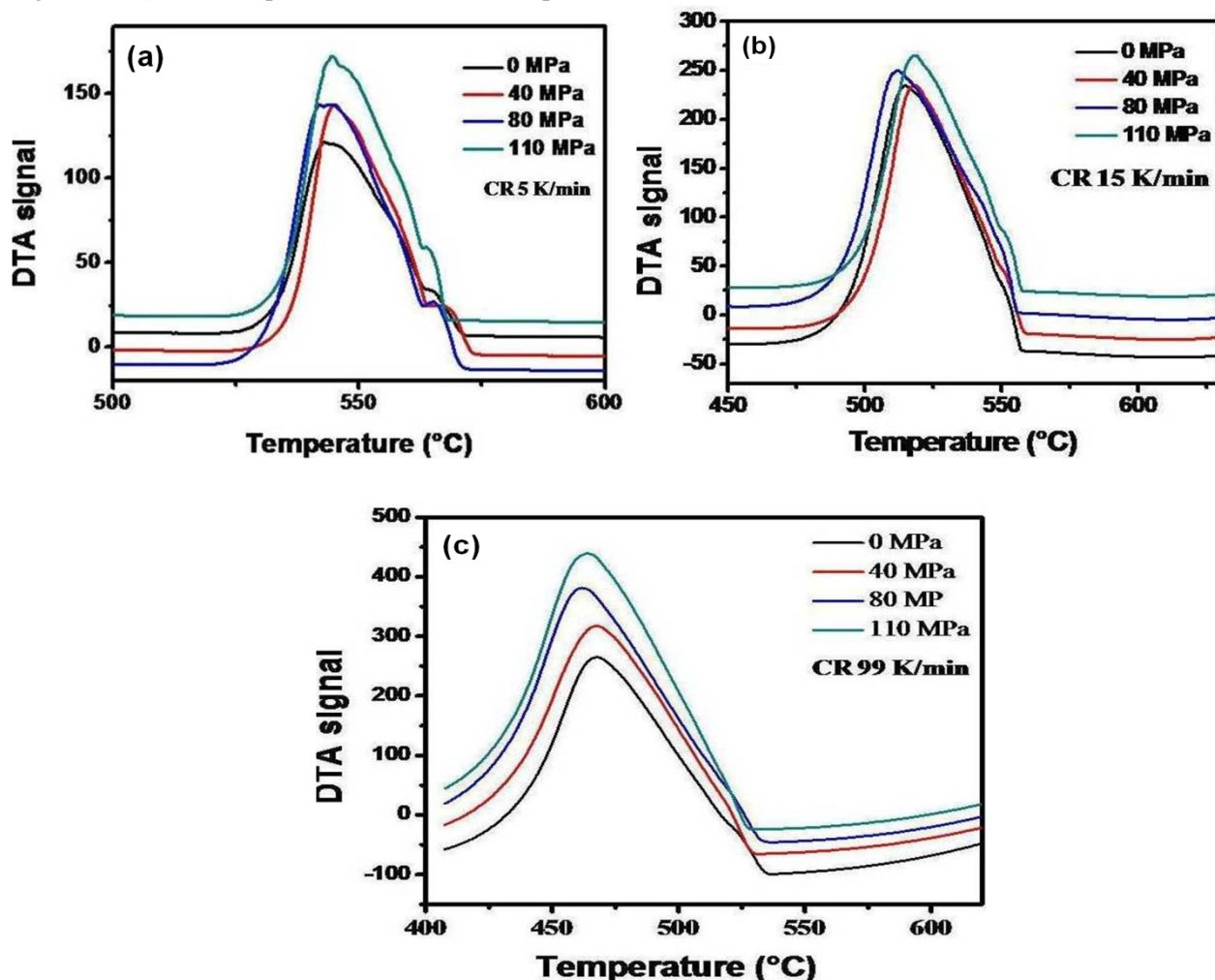


Fig.3: DTA analysis of cooling rates of specimens squeeze cast at different specific pressures. (DTA thermogram was separated along the y-axis)

The application of pressure causes greater cooling rates for the solidifying alloy which can be realized due to reduction in the air gap between the melt and the die wall. Obviously, the increase of the under cooling degree and heat-transfer coefficient will result in the refinement of the grain size of squeeze casting alloy. As a result the specimen structure becomes thinner, finer and more homogenous [29] (see Fig.1). The same results are confirmed by LI Run-xia et al [30] and Boschetto A [31]. Thus, the morphology of eutectic Si plays a vital role determining the mechanical properties of Al–Si alloy.

Table 2: Temperature (°C) of exothermic peaks corresponding to DTA curves

Pressure(MPa)	Peak 1			Peak 2		
	5 K/min	15 K/min	99 K/min	5 K/min	15 K/min	99 K/min
0 MPa	562	549	521	542	513	465
40 MPa	563	550	-	545	517	559
80 MPa	563	547	-	542	510	475
110 MPa	562	550	-	544	517	472

3.2 Effect of cooling rate on solidification behavior of Al-11%Si.

The cooling curves recorded for samples of gravity cast (P=0MPa) Al-11%Si alloy at various cooling rates are shown in Fig.4. In Table 3, there are mainly three solidification reactions in Al-11%Si alloy. Peak 1 and peak 2 represent the development of aluminium dendrites and the main binary eutectic reaction. It is seen that formation temperatures of the various phases are changed when the cooling rate is increased. The shift magnitude increases with the increase of the cooling rate. This shift changes the characteristic parameters of thermal analysis particularly in the liquidus region. The cooling rate is proportional to the heat extraction from the sample during solidification. Therefore, when the cooling rate is 5 (k.min⁻¹) there are two solidification reactions for this alloy. From the sample the rate of heat extraction is slow and the slope of the cooling curve is small. So, it creates a wide cooling curve. But, when the cooling rate increases to 15 K/min the peak 1 becomes small and eventually disappeared at high cooling rate to 99 K/min.

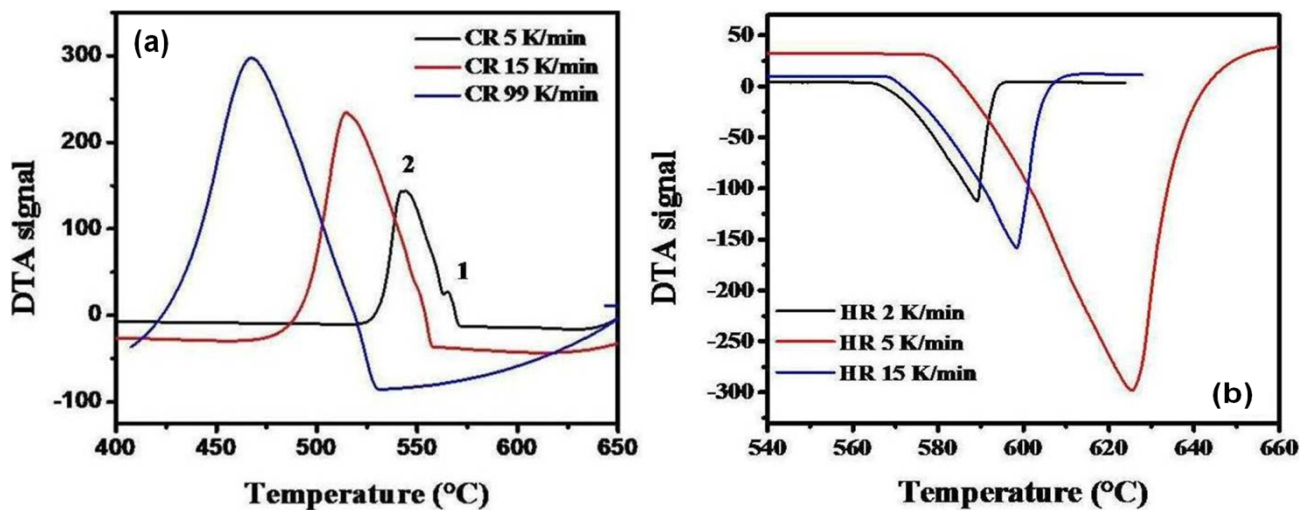


Fig.4: Cooling and heating curves of Al-11%Si alloy of gravity cast (P=0 MPa).

Table 3: DTA cooling characteristics of as-cast Al-11%Si alloy

Cooling rate K/min	Temperature of peak 1/°C		Temperature of peak 2/°C	
	Onset	Peak	Onset	Peak
5	570.17	565.50	562.76	543.31
15	557.73	552.27	548.38	514.51
99	-	-	528.54	567.01

Three micrographs from samples Al-11%Si alloy cooled with cooling rate: 5, 15 and 99 K/min are shown in Fig. 5. The microstructures of the alloy showed the presence of eutectic silicon and (Al) matrix and intermetallic phases such as Al₅FeSi (β -phase), and Al₂Cu (Cu rich phase). It is evident from this results that the increase of cooling rate causes a decrease in the grain size and the secondary dendrite arm spacing (SDAS). As seen on the fig.6 that from 5 K/min to 15 K/min then to 99 K/min, average SDAS was decreased to finer scale and was found as 137.66±1, 83.07±1 and 71.74±2 μ m, respectively. Similar result of SDAS of ACA1Si9Cu aluminum alloy was reported in literature Dobrzański et al. [32]. Besides, the increasing of cooling rates causes the increase of constitutional under cooling. This condition causes the formation of more secondary dendrite arms. In addition, increasing the cooling rate causes the interface of the liquid and solid to move faster [33]. Consequently, ratio of area to volume of dendrite arms should increase in order to facilitate the heat extraction. Also, the increase of dendrite thickness is formed because of ripening and coalescence which needs diffusion and time. As a result the specimen structure becomes thinner and finer.

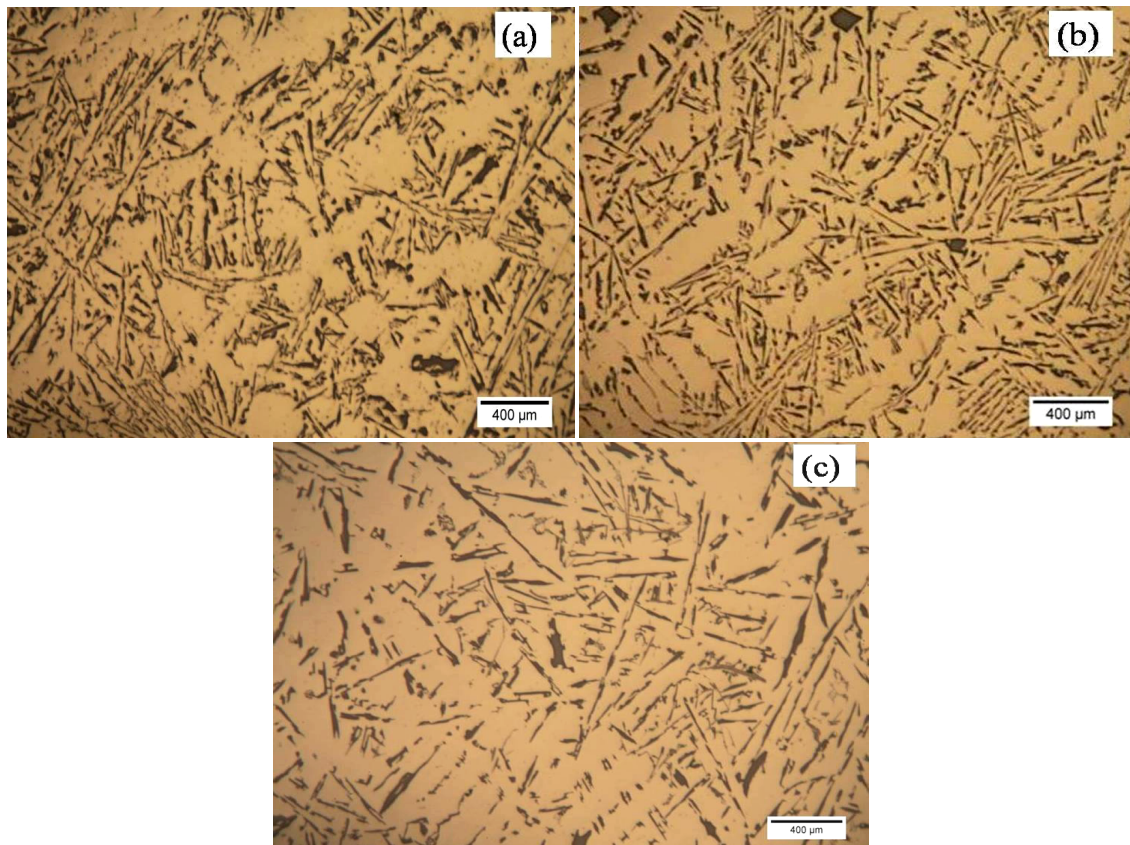


Fig.5: Microstructure of the primary and eutectic silicon particles at different cooling rates (a) =5 K/min, (b) = 15 K/min, (c) =99 K/min.

The results of SEM are confirmed with optical microscope for identification of these intermetallic phases. SEM micrographs have shown that the θ - Al_2Cu phases (the clearest phase) are around the very fine needles of β - Al_5FeSi phase. Figure 7 illustrates the influence of cooling rate on the morphology of Al_5FeSi phase. It is seen that high cooling rate reduced the size of beta phase precipitates. The beta phase appears shorter and more homogeneous in length and volume fraction, as illustrated in this figure. The effect of cooling rate on beta phase size is consistent with other reported studies By Khalifa et al. [34] and Narayanan et al. [35].

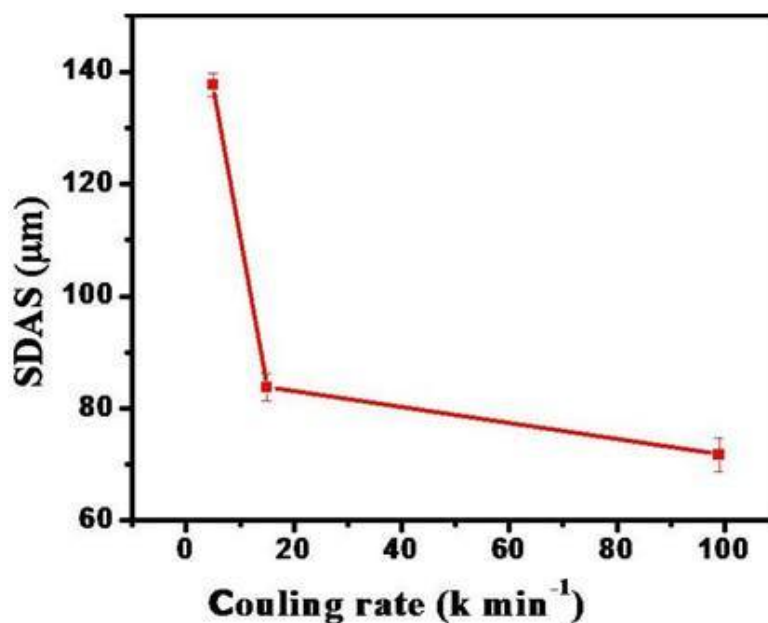


Fig.6: Variation of SDAS as a function of cooling rate.

In current experiments, the results revealed that as the cooling rate increases some nucleation sites for the beta phase appeared in the bulk that were distributed evenly within the sample away from the skin as seen in Fig.7(a). However at high cooling rate, it might be that part of the precipitated beta plates did not have enough time to get full extension. The needle-shaped β phases have negative effects on the mechanical properties. Yet, the existence of the θ phase and the refinement of α -Al phase caused an improvement in the mechanical properties [36].

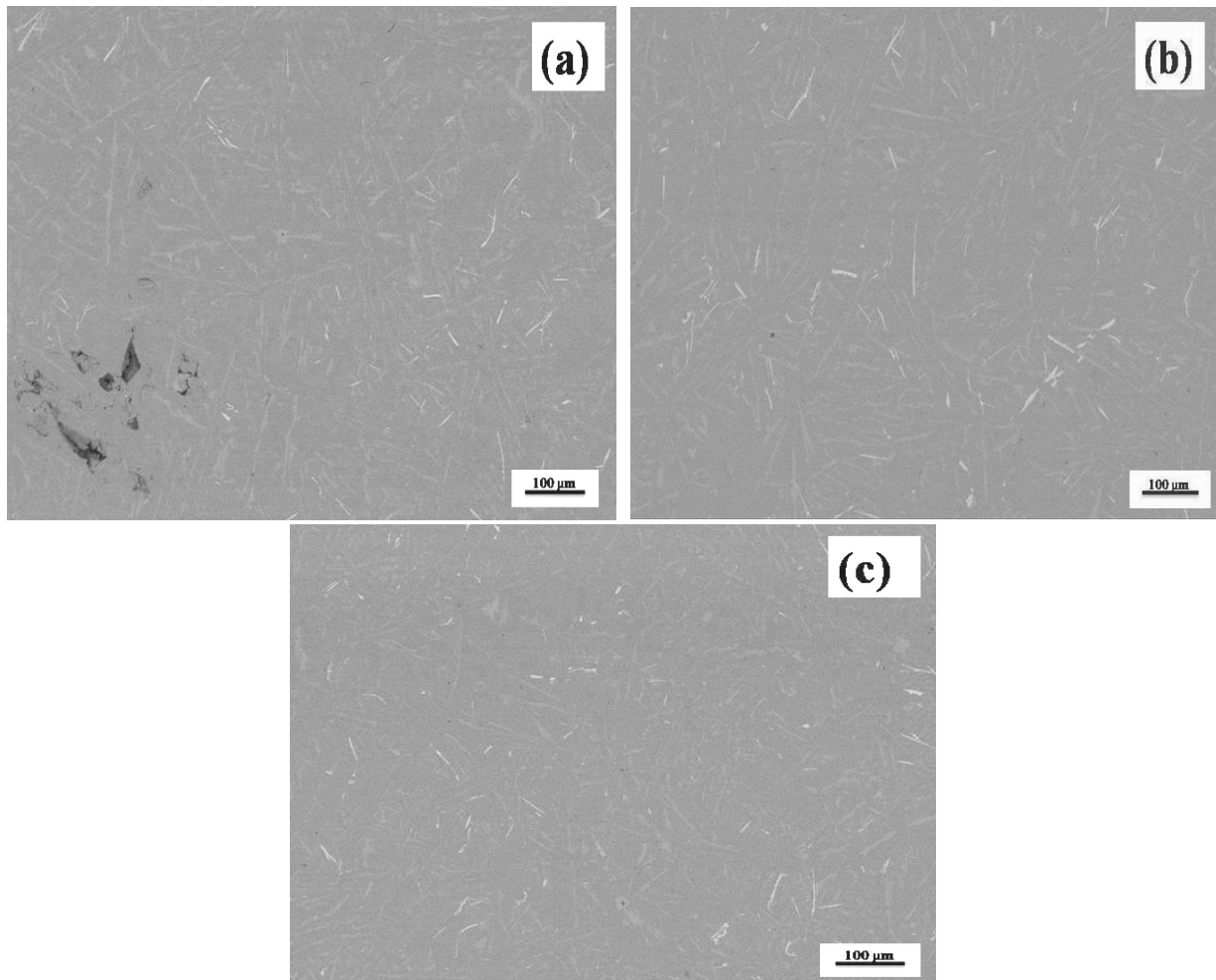


Fig. 7: SEM micrographs of DTA samples cooled at various cooling rates (a) 5 K/min, (b) 15 K/min, (c) 99 K/min. Beta phase appear in light contrast.

3.3 Mechanical Properties

The data of mechanical properties (ultimate tensile UTS (MPa), yield strength YS (MPa), elongation (%) and micro-hardness (HV)) of this alloy in various pressures of the as-cast are shown in table 4. It can be seen from this table that the typical tensile properties of the alloy increases with increasing applied pressure.

The results found that the UTS increase from 202 ± 1 to 231 ± 1 MPa with the squeeze pressure of 40 to 110MPa, respectively. As for the elongation values increases remarkably at 110 MPa compared to gravity die casting. The same results, agree quite well with the results reported in the literature [6, 11].

It also shown Vickers microhardness values increased from 62 ± 2 HV to 72 ± 2 HV for the samples when the applied pressure from 0 to 110 MPa, respectively. These micro-hardness values found in this study are comparable by Abou El-Khair [11].

It is well known that the mechanical properties of cast specimens are dependent in the first one, the existence of entrapped gas or shrinkage pores. In the second one, the large needle-like iron aluminide intermetallic compounds, uniform grains, and SDAS values throughout the region. However, in this study, The application of pressure

causes greater cooling rates for the solidifying alloy which can be realized due to reduction in the air gap between the metal and the die surface. Obviously, the increase of the under cooling degree and heat-transfer coefficient will result in the refinement of the grain size of squeeze casting alloy as a result the specimen structure becomes thinner and finer. This gives elevation to the improved tensile strength on the one hand and on the other hand desirable ductility.

Table 4: Tensile properties and microhardness of the Al-11%Si alloy in various pressures

Pressure (MPa)	UTS (MPa)	YS (MPa)	Elongation (%)	HV (0.3)
0	198±1	58±1	2.8±2	62±2
40	202±1	78±1	1.8±2	64±2
80	217±1	74±1	3.2±2	68±2
110	231±1	134±1	6.8±2	72±2

Conclusion

The effect of the cooling rate on the structural features and thermal analysis characteristic were examined. The results are summarized as follows:

1. The results of DTA show that the primary reaction is promoted in squeeze cast Al-11%Si alloy solidified at high pressure and the fine microstructure is obtained with the increase of pressure.
2. The solidification of Al-11%Si cast alloy commenced with precipitation of primary silicon phase. Then it progressed with formation of the (α (Al) + β (Si)) eutectic. Finally, at 542°C the solidification of β intermetallic phase was detected at the end of solidification process on the DTA cooling curves.
3. Differential Thermal Analysis reported that the Al-Si eutectic depression increases with the cooling rate as expected, though only values of cooling rate higher than 15 K/min relate to satisfactory modification of squeeze cast Al-11%Si alloy.
4. Increasing the cooling rate from 5 K/min to 99 K/min refines all microstructural features including decreases Secondary Dendrite Arm Spacing (SDAS) from 137.66±1 μm to 71.74±2 μm , intermetallic compounds and improves silicon modification. Similar result was reported in literature Dobrzański et al. [33]. That caused an improvement in the mechanical properties.

Acknowledgement-We wish to thank Dr. Jacques Lacaze of Center for Interuniversity Research and Materials Engineering Toulouse CIRIMAT – INP-ENSIACET, Toulouse for his assistance with some of the measurements during the author's stay there. One of the authors, Henda Barhoumi would like to acknowledge very much, the Tunisian Ministry of Higher Education and Scientific Research for its financial support.

References

1. M. P. Jahan, K. Pegah, E.L. M. Kwang, M. Rahman, Y. S. Wong, *Int J Adv Manuf Technol.* 78 (2015) 1127.
2. V.A. Hosseini, S.G. Shabestari, R. Gholizadeh, *Mater Des.* 50 (2013) 7.
3. S. Hegde, K.N. Prabhu, *J Mater Sci.* 43 (2008) 3009.
4. H. Liao, Y. Sun, G. Sun, *Materials Science and Engineering A.* 335 (2002) 62.
5. M. M. Hague, M. A. Malegue, *Journal of Materials Processing Technology,* 77 (1998) 122.
6. S. Souissi, M. Ben Amar, C Bradai, *Int J Mater Form.* 6 (2013) 249.
7. P. Vijian, V. P. Arunachalam, *J Mater Proces Tech.* 170, (2005) 32-36.
8. M. S. Yong, A. J Clegg, *J Mater Proces Tech.* 145 (2004) 134–141
9. S.M. Skolianos, G. Kiourtsidis, T. Xatzifotiou, *Mater Sci Eng.* 231 (1997) 17.
10. C.H. Fan, Z.H. Chen, W.Q. He, J.H. Chen, D. Chen, *J Alloys Compd.* 504 (1997) 42
11. A. El-Khair, *Mater Letts.* 59 (2005) 894
12. E. Hajjari, M. Divandari, *Mater Des.* 29 (2008) 1685.
13. A. Mohamed, A. Samuel, F. Samuel, H. Doty, *Mater Des,* 30 (2009) 3943.
14. M. Zeren. *Mater. Des.* 28 25 (2007) 11–7
15. Z. Ma, E. Samuel, A. Mohamed, A. Samuel, F. Samuel, H. Doty, *Mater Des.* 31 (2010) 902–12.
16. S. Gowri, *AFS Trans.* 102 (1994) 503-508.

17. K. Radhakrishna, S. Seshan, M.R. Seshadri, *AFS Trans.* 88 (1980) 695-701.
- 18 M. C. Flemings, T. Z. Kattamis, B. P. Bardes, *AFS Trans.* 99 (1991) 501-506
19. A. M. Figueredo, Y. Sumartha, M. C. Flemings. *Light Metals*, B. Welch, ed., *The Minerals, Metals and Materials Society*, 1103-1106 (1998)
20. Easton M A, StJohn D H. *Mater Sci Eng A* 486 (2008) 8-13.
21. K. Radhakrishna, S. Seshan, *Cast Metals* 2 (1989) 34-38
22. Y. C. Lee, A. K. Dahle, D. H. StJohn, J. E. C. Hutt, *Mater Sci Eng A*, 259 (1999) 43-52.
23. M. Srecko, R. Radomir, M. Srdjan, A. Zagorka, R. Karlo. *Intermetallics* 19 (2011) 486-492.
24. M. Dehnavi, M. Kuhestani, M. Haddad-Sabzevar, *Metall. Mater Eng*, 21(2015) 95-205.
25. M. Zeren, *J Mater Process Technol* 169 (2005) 292-298.
26. S. G. Shabestari, S. Ghodrat, *Mater Sci Eng A*. 467 (2007) 150–8.
27. S. Kores, M. Voncina, B. KOsec, J. Medved, *Metallurgija* 51 (2012) 216-220
28. D. Ferdian, B. Suharno, B. Duployer, C. Tenailleau, L. Salvo, J. Lacaze. *Trans Indian Inst Met* 65(6) (2012) 821-825
29. A. CLEGG, *Foundry Trade Journal* 166 (1993) 484-485
30. L.I. Run-xia, L.I. Rong-de, B.A.I. Yan-hua, Q.U. Ying-dong, Yuan Xiao-guang, *Trans Nonferrous Met Soc China* 20 (2010) 59-63.
- 31 A. Boschetto, G. Costanza, F. Quadrini, M.E. Tata. *Mater Lett* 61 (2007) 2969–2972
32. L. A. Dobrzański, R. Maniara, J. H. Sokolowski, *AMSE*. 28 (2007) 105-112.
33. S.G. Shabestari, M. Malekan. *J Can Metall Q* 44 (2005) 305–12.
34. W. Khalifa, F. H. Samuel, J. E. Gruzleski, *Metall. Mater. Trans. A* 34 (2003) 807 –825
35. L. A. Narayanan, F. H. Samuel, J. E. Gruzleski, *Metall. Mater. Trans. A* 25 (1994) 1761-1773.
36. M. V. Kral, H. R. McIntyre, *Scripta Mater.* 51 (2004) 215–219.

(2019) ; <http://www.jmaterenvironsci.com>